Viscoelastic behavior of polymer melt in rapidly oscillating plates : an application of multiscale modeling (Mathematical Analysis in Fluid and Gas Dynamics)

AUTHOR(S):

Yasuda, Shugo; Yamamoto, Ryoichi

数理解析研究所講究録
第1690巻 2010年 21-28

Viscoelastic behavior of polymer melt in rapidly oscillating plates: an application of multiscale modeling

S. Yasuda and R. Yamamoto
Department of Chemical Engineering,
Kyoto University

Dedicated to Professor Kenji Nishihara on his 60th birthday

abstract

The behavior of supercooled polymer melt composed of short chains with ten beads between rapidly oscillating plates is simulated by using a hybrid simulation of molecular dynamics and computational fluid dynamics. The flow profiles of polymer melt near an oscillating plate are quite different from those of Newtonian fluid. The viscous boundary layer of the melt is much thinner than that of the Newtonian fluid due to the shear thinning of the melt. Three different rheological regimes, i.e., the viscous fluid, viscoelastic liquid, and viscoelastic solid regimes, form over the oscillating plate according to the local Deborah numbers. The melt behaves as a viscous fluid when $\omega\tau^R \lesssim 1$, and the crossover between the liquid-like and solid-like regime takes place around $\omega\tau^\alpha \simeq 1$ (where ω is the angular frequency of the plate and τ^R and τ^α are Rouse and α relaxation time, respectively).

1 Introduction

A lot of products in our daily lives contain soft matters (e.g. colloids, polymers, and liquid crystals). One of the most unique characters of soft matters is that they exhibit both solid- and liquid-like responses to mechanical strains or shape deformations. When computer simulations of fluids are performed, either computational fluid dynamics (CFD) or molecular dynamics (MD) is usually employed. In the case of CFD, mechanical properties of fluids must be modeled mathematically in advance as a form of "constitutive relation" to be used in simulations. CFD is thus valid only for the cases in which both mechanical properties of fluids and the flow profiles are not too complex. Polymer melts, however, have very complicated mechanical properties in general, and their flow profiles are complex in rapidly oscillating plates. In the case of MD simulation in contrast, fluids consist of huge numbers of molecules of arbitrary shapes. It is thus applicable for any flows of any complex fluids in principle. However,

the drawback here is enormous computational time required to resolve the dynamics of all the molecules consist of fluids. Hence, MD simulation is not yet applicable to problems which concern large scale motions far beyond the molecular size, as is done in the present study. (An expected time to simulate only a gram of fluid would exceed one hundred years even if the rapid progress of computer continues forever.) In order to overcome this difficulty, we have recently developed a hybrid simulation of MD and CFD based on a local sampling strategy, in which the macroscopic dynamics are solved using a CFD scheme but, instead of using any constitutive equations, a local stress is calculated by using a non-equilibrium MD simulation associated with each lattice node of the CFD computation.[1] The basic idea of the hybrid simulation method was put forward earlier by Kevrekidis *et al.*[2] and also by Ren and E.[3]

In previous papers, the validity of the hybrid methods and their efficiencies are examined intensively for viscous fluids without memory effects. De *et al.* have recently proposed a new hybrid method, which is called the scale bridging method in their paper, that can correctly reproduce the memory effect of the polymeric liquid, and performed a simulation of a non-linear viscoelastic polymeric liquid between oscillating plates.[4] They have also compared the results obtained by the scale bridging method with those obtained by a full MD simulation, thereby demonstrating validity of the method. In the present letter, we also model the behavior of polymer melt between oscillating plates by using the same strategy of multiscale modeling, but we focus on the complex rheology of a supercooled polymer melt in the viscous diffusion layer that arises near an rapidly oscillating plate. The boundary layer arises if the width between plates is much larger than the thickness of viscous diffusion layer. Note that, in Ref. [4], the thicknesses of viscous diffusion layers are estimated to be comparable to the widths of the plates[5], thus the boundary layers are not clearly seen.

In the present problem, the macroscopic quantities are quite non-uniform, and two different characteristic length scales appear that must be resolved; one is that of a polymer chain and the other is that of a boundary layer arising near the oscillating plate. This problem constitutes an important application of multiscale modeling since it is quite difficult to solve this problem by using a full MD simulation because the length of the boundary layer is much larger than that of a polymer chain. In the following, we briefly state the problem and outline the hybrid simulation method, and then discuss the numerical results. Finally we give a summary of our conclusions.

2 Problem and multiscale modeling

We consider a polymer melt with a uniform density ρ_0 and a temperature T_0 between two parallel plates (see Fig. 1(a)). The upper- and lower-plate start to oscillate in opposite, parallel directions with a constant frequency ω_0 at t=0. The polymer melt is composed of short chains with ten beads. All of the bead particles interact with a truncated Lennard-Jones potential defined by[6] $U_{\rm LJ}(r) = 4\epsilon\left[(\sigma/r)^{12} - (\sigma/r)^6\right] + \epsilon$ for $r \le 2^{1/6}\sigma$, and 0 for $r > 2^{1/6}\sigma$. By using the repulsive part of the Lennard-Jones potential only, we may prevent spatial overlap of the particles. Consecutive beads on each chain are connected by an anharmonic spring potential, $U_{\rm F}(r) = -\frac{1}{2}k_c R_0^2 \ln\left[1 - (r/R_0)^2\right]$, with k_c=$30\epsilon/\sigma^2$ and R_0=1.5σ. The number density of the bead particles is fixed at

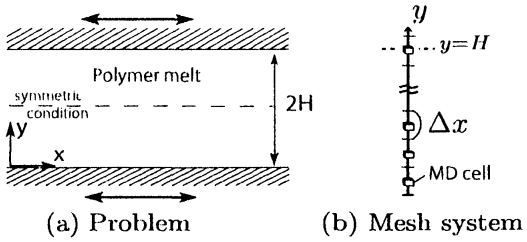

Figure 1: Schematics for the problem and mesh system.

$\rho_0/m=1/\sigma^3$, where m is the mass of the bead particle. With this number density the configuration of bead particles becomes severely jammed at a low temperature, resulting in the complicated non-Newtonian viscosity and long-time relaxation phenomena typically seen in glassy polymers. In the present letter, we fix the temperature at $T=0.2\epsilon/k$, where k is the Boltzmann constant.[7]

We assume that the macroscopic quantities are uniform in the x- and z-directions, i.e., $\partial/\partial x=\partial/\partial z=0$. Then the macroscopic velocity v_α is described by the equations, $\rho_0 \partial v_x/\partial t = \partial \sigma_{xy}/\partial y$ and $v_y=v_z=0$, where $\sigma_{\alpha\beta}$ is the stress tensor. Here and afterwards, the subscripts α, β, and γ represent the index in Cartesian coordinates, i.e., $\{\alpha,\beta,\gamma\}=\{x,y,z\}$. We also assume the non-slip boundary condition at the oscillating plate, $v_x=v_0 \cos\omega_0 t$ at $y=0$ (where v_0 is a constant amplitude of the oscillation velocity), and the symmetric condition at $y=H$ (i.e., $v_x(y=H+\Delta x/2)=-v_x(y=H-\Delta x/2)$). If the frequency ω_0 is large enough, the thin viscous boundary layer forms over the oscillating plate. The thickness of the layer is estimated, for fluids with a constant viscosity ν_0, as $l_\nu \sim 7\sqrt{\nu_0/\omega_0}$. Note that the thickness of the viscous layer l_ν is much smaller than the width between the plates, $l_\nu \ll H$, but is usually much larger than the scale accessible to a full MD simulation, in which the characteristic length scale is the length of the polymer chain l_p, $l_\nu \gg l_\mathrm{p}$.

The constitutive relation of the stress tensor is quite complicated[8, 9]; the temporal value of the stress tensor of a fluid element depends on the previous values of the velocity gradients of the fluid element. The relation may be written in a functional form as,

$$\sigma_{\alpha\beta}(t, x_\alpha) = F_{\alpha\beta}[\kappa_{\alpha\beta}(t', x'_\alpha(t'))], \quad \text{with} \quad t' \le t, \tag{1}$$

where $\kappa_{\alpha\beta}$ is the velocity gradient, $\kappa_{\alpha\beta} = \partial v_\alpha/\partial x_\beta$, and $x'_\alpha(t')$ represents the path line along which a fluid element has been moving. In the one-dimensional problem, however, we don't need to consider the path line of the convective fluid element since the macroscopic velocity is restricted to be only in the x-direction where the macroscopic quantities are assumed to be uniform. Thus the stress tensor for the present problem may be written in a functional involving the local strain rate,

$$\sigma_{\alpha\beta}(t, y) = F_{\alpha\beta}[\dot\gamma(t', y)], \quad \text{with} \quad t' \le t, \tag{2}$$

where $\dot\gamma$ is the strain rate, $\dot\gamma=\partial v_x/\partial y$. Note that, although Eq. (2) becomes much simpler than Eq. (1), the temporal value of the local stress still depends on the previous values of the local strain rate. Its dependence is quite complicated, especially for glassy materials (for which explicit formulas are unknown in general). In our hybrid

simulation, instead of using any explicit formulas for the constitutive relation, the local stress is generated by the non-equilibrium MD simulation associated with each local point. See Fig. 1 (b).

We briefly explain our hybrid simulation method. The computational domain $[0,H+\Delta x/2]$ is divided into thirty-two slits with a constant width Δx. We use a usual finite volume method with a staggered arrangement, where the velocity is computed at the mesh node and the stress is computed at the middle of each slit. One hundred chains are confined in each cubic MD cell with a side length $l_{\rm MD}=10\sigma$. As for the time-integration scheme, we use the simple explicit Euler method with a small time-step size Δt. The local stress at each time step of the CFD is calculated by performing a non-equilibrium MD simulation according to the local strain rate in each MD cell. The techniques of the non-equilibrium MD simulation are the same as those in the previous paper[1]; we use the Lees-Edwards sheared periodic boundary condition and a Gaussian iso-kinetic thermostat to keep a constant temperature. In the present problem, however, we cannot assume a local equilibrium state at each time step of the CFD simulation since the relaxation time of the stress may become much longer than the time-step size of the CFD simulation (in which the macroscopic motions of the system should be resolved). In the present simulations, the simple time-average of the temporal stresses of the MD (averaged over the duration of a time-step of the CFD simulation) are used as the stresses at each time step of the CFD calculation without ignoring the transient time necessary for the MD system to be in steady state. The final configuration of molecules obtained at each MD cell is memorized as the initial configuration for the MD cell at the next time step of the CFD. Thus we trace all of temporal evolutions of the microscopic configurations with a microscopic time step so that the memory effects can be reproduced correctly. Note that, compared with a full MD simulation, we can achieve an efficient computation with regard to the spatial integration by using MD cells that are smaller than the slit size used in the CFD simulation. The efficiency of the performance of our hybrid simulation is represented by the ratio of the slit size used in the CFD model Δx to the cell size of the MD simulation $l_{\rm MD}$, $\Delta x/l_{\rm MD}$. Hereafter, the quantities normalized by the units of length σ and time $\tau_0=\sqrt{m\sigma^2/\epsilon}$ are denoted with a superscript "*". In the following simulations, we fix the time-step size of the CFD simulation Δt, sampling duration of the MD simulation $t_{\rm MD}$ and time-step size of the MD simulation $\Delta\tau$ as $\Delta t^*=t^*_{\rm MD}=1$ and $\Delta\tau^*=0.001$, respectively. Thus, one thousand MD steps are performed in each MD cell at each time step of the CFD computation.

3 Result and discussion

We perform the hybrid simulations for two cases: Case A, in which $\omega_0^*=2\pi/256$ and $H^*=787.5$, and Case B, in which $\omega_0^*=2\pi/1024$ and $H^*=1575$. The amplitude of the oscillation velocity is fixed as $v_0^*=10$ in both cases. The widths of the slits are $\Delta x^*=25$ for Case A and $\Delta x^*=50$ for Case B, and the ratios of the mesh size of the CFD Δx to the cell size of the MD $l_{\rm MD}$ are $\Delta x/l_{\rm MD}=2.5$ for Case A and 5 for Case B. Figure 2 shows the instantaneous velocity profiles near an oscillating plate over a period for (a) Case A and (b) a Newtonian fluid with a constant viscosity $\nu_0^*=53$, which corresponds

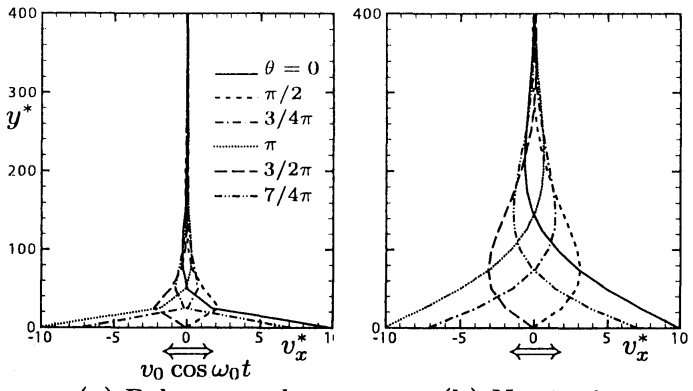

(a) Polymer melt (b) Newtonian

Figure 2: The velocity profiles near an oscillating plate at $\omega_0 t$=240π+θ, θ/π=0, 1/2, 3/4, 1, 3/2, and 7/4, for ω_0^*=2π/256. (a) The result for the polymer melt and (b) that for a Newtonian fluid. The vertical axis represents the height y and the horizontal axis the velocity v_x.

to the dynamic viscosity of the model polymer melt for Case A. The dynamic viscosity is calculated via G_2^*/ω_0 (where G_2 is the loss modulus in the linear regime). It is seen that the boundary layer of the melt is much thinner than that of the Newtonian fluid. This is caused by the shear thinning; the local loss modulus near the boundary is, as we see below, much smaller than that for the linear regime, thus the thickness of the viscous diffusion layer becomes thinner than that for the Newtonian fluid.

We also measure the local viscoelastic properties in terms of the local storage modulus $G_1(y)$ and loss modulus $G_2(y)$. It should be noted that the local macroscopic quantities oscillate with a different phase retardation at each different point. The local moduli are calculated in the following way: The discrete Fourier transforms of the temporal evolutions of the strain γ, $\gamma(t,y) = \int_0^t \dot{\gamma}(t',y)dt'$, and shear stress σ_{xy} during the steady oscillation states are performed. The discrete Fourier transformations are written as $\hat{g}_k^l = \frac{1}{N+1}\sum_{n=0}^{N} g_n^l \exp(\mathrm{i}2\pi nk/(N+1))$, with g_n^l=$g(n\Delta t, l\Delta x)$ (n=0,...,N and l=0,...,32) , where g represents the strain or shear stress (e.g., g=γ or σ_{xy}). By using the Fourier coefficients for the mode of the oscillating plate k_0, k_0=1+($\omega_0/2\pi$)N, the time evolution of the local strain at y=y^l can be expressed as a cosine function,

$$\gamma^l(t) = \gamma_0^l \cos(\omega_0 t + \delta^l), \tag{3}$$

with $\gamma_0^l = \sqrt{(\hat{\gamma}'^l_{k0})^2 + (\hat{\gamma}''^l_{k0})^2}$ and $\delta^l = \tan^{-1}(\hat{\gamma}''^l_{k0}/\hat{\gamma}'^l_{k0})$. Hereafter the superscripts "$\prime$" and "$\prime\prime$" indicate the real and imaginary part of the discrete Fourier coefficients, respectively. The time evolution of the local shear stress can also be expressed as

$$\sigma_{xy}^l(t) = \sigma_1^l \cos(\omega_0 t + \delta^l) - \sigma_2 \sin(\omega_0 t + \delta^l), \tag{4}$$

with $\sigma_1^l = \hat{\sigma}'^l_{k_0} \cos\delta^l + \hat{\sigma}''^l_{k_0} \sin\delta^l$ and $\sigma_2^l = \hat{\sigma}''^l_{k_0} \cos\delta^l - \hat{\sigma}'^l_{k_0} \sin\delta^l$. Thus, the local storage modulus G_1 and loss modulus G_2 are written, respectively, as $G_1(y^l)$=σ_1^l/γ_0^l and $G_2(y^l)$=σ_2^l/γ_0^l.

Figure 3 shows the spatial variations of the local storage modulus and loss modulus and the amplitude of the local strain for Case A. The shear thinning is seen near the

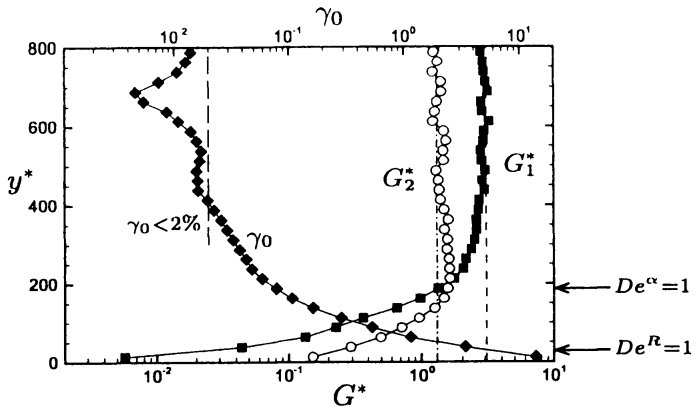

Figure 3: The spatial variations of the local moduli G_1 and G_2 (lower axis) and the amplitude of the local strain γ_0 (upper axis) for Case A. The dashed and dash-dotted lines show the values of G_1 and G_2 for the linear regime (G_1^*=3.1 and G_2^*=1.3), respectively. The linear moduli are calculated by the non-equilibrium MD simulations with small strains for 0.005< γ_0 <0.01. The long-dashed line represents γ_0=2%. The left arrows on the right-side vertical axis show the positions where the local Deborah numbers, shown in Fig. 5, are equal to unity.

plate; the strain γ_0 (or the strain rate $\dot{\gamma}_0=\omega_0\gamma_0$) is quite large near the oscillating plate and both moduli are much smaller than those for the linear regimes. In the close vicinity of the oscillating plate, the storage modulus G_1 is much smaller than the loss modulus G_2, $G_1 \ll G_2$. Hence, the melt behaves as a viscous fluid. The storage modulus rapidly grows with the distance from the oscillating plate, and the viscoelastic crossover occurs at $y^* \sim 200$. Both moduli attain their linear values, which are shown as dashed and dot-dashed lines in Fig. 3, for distance that is far from the oscillating plate where the local strains are less than about two percent. The overall features are also consistent with Case B, although the crossover is not as clear as that in Case A (See Fig. 4). Thus, the local rheology of the melt can be divided into three regimes, i.e., the viscous fluid, viscoelastic liquid, and viscoelastic solid regimes. These regimes may be also characterized by the two "local" Deborah numbers. One is defined by the local Rouse relaxation time τ_R of the melt and the angular frequency of the plate ω_0, $De^R=\omega_0\tau_R$, and the other is defined by the local α relaxation time τ_α and the angular frequency ω_0, $De^\alpha=\omega_0\tau_\alpha$. Note that the local Rouse and α relaxation times vary according to the local strain rate $\dot{\gamma}$, $\tau = \tau(\dot{\gamma})$. Figure 5 shows the spatial variation of the local Deborah number De^R and De^α, where the local relaxation times τ_R and τ_α are calculated by substituting the values of $\dot{\gamma}_0^l$, which are obtained via Eq. (3), into the fitting functions for the relaxation times for the simple shear flows obtained in Ref. [7]. In Figs. 3 and 4, the positions at which the local Deborah numbers become equal to unity are shown by the left arrows. It is seen that the melt behaves as a viscous fluid, $G_2 \gg G_1$, for $De^R \lesssim 1$, while the viscoelastic properties become pronounced for $De^R \gtrsim 1$. This is consistent with the rheology diagram for a model polymer melt obtained in Ref. [10]. It is also seen that the crossovers of the liquid-like regime, $G_2 > G_1$, and the solid-like regime, $G_1 > G_2$, take place at $De^\alpha \sim 1$.

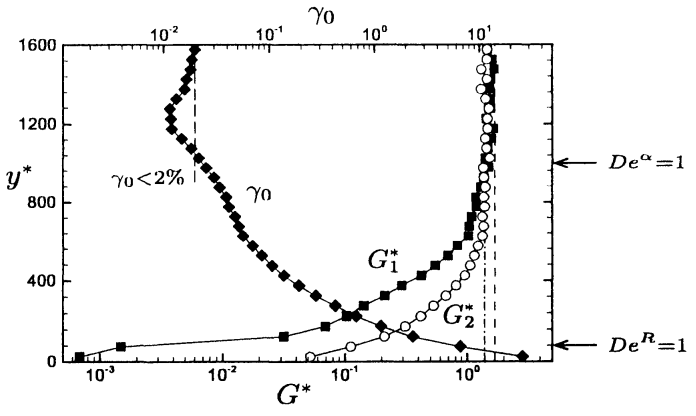

Figure 4: The spatial variations of the local moduli G_1 and G_2 (lower axis) and the amplitude of the local strain γ_0 (upper axis) for Case B. The dashed and dash-dotted lines show the values of G_1 and G_2 for the linear regime (G_1^*=1.7 and G_2^*=1.4), respectively. See also the caption for Fig. 3.

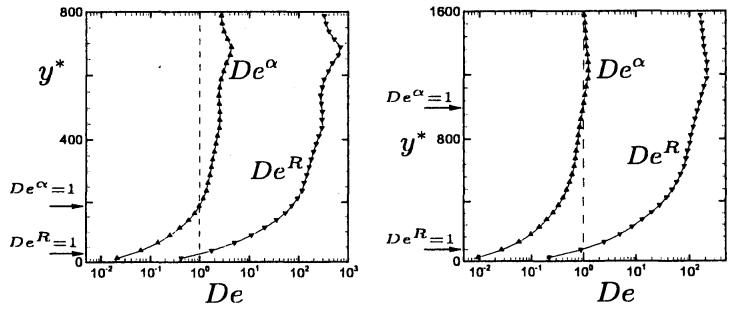

(a) $\omega_0 = 2\pi/256$ (b) $\omega = 2\pi/1024$

Figure 5: The local Deborah numbers (defined via the Rouse relaxation time τ_R and the α relaxation time τ^α) $De^R = \omega_0\tau_R$ and $De^\alpha = \omega_0\tau^\alpha$. (a) Case A. (b) Case B. The right arrows on the y-axis show the position where the Deborah numbers are equal to unity.

4 Summary

The behavior of supercooled polymer melt between rapidly oscillating plates is simulated by using a hybrid simulation of MD and CFD. In our simulation, the memories of molecular configurations of the fluid elements are correctly traced at the microscopic level. The efficiency of our hybrid simulation is represented by the ratio of the mesh size of the CFD simulation Δx to the cell size of the MD simulation l_{MD}. In the present simulations, $\Delta x/l_{\mathrm{MD}}$=2.5 for Case A and 5 for Case B. The flow profiles of polymer melt are quite different from those of Newtonian fluid with a dynamic viscosity of the model polymer melt. The shear thinning of polymer melt takes place near the oscillating plate, and thus the boundary layer of the polymer melt becomes much thinner than that of the Newtonian fluid. The local rheology of the melt also varies considerably in the viscous boundary layer, so that three different regimes, i.e., the viscous fluid, viscoelastic liquid, and viscoelastic sold regimes, form between the oscillating plates.

It is also found, in the viscous fluid regime, that the local Deborah number defined via the Rouse relaxation time and the angular frequency of the plate is less than about unity, $De^R \lesssim 1$. The crossover between the liquid-like and solid-like regimes takes place around the position where the local Deborah number defined via the α relaxation time and the angular frequency is equal to unity, $De^\alpha \sim 1$.

References

[1] S. Yasuda and R. Yamamoto, Phys. Fluids **20**, 113101 (2008).

[2] I. G. Kevrekidis, C. W. Gear, J. M. Hyman, P. G. Kevrekidis, O. Runborg, and C. Theodoropoulos, Comm. Math. Sci. **1**, 715 (2003).

[3] W. Ren and W. E, J. Compt. Phys. **204**, 1 (2005).

[4] S. De, J. Fish, M. S. Shephard, P. Keblinski, and S. K. Kumar, Phys. Rev. E **74**, 030801(R) (2006).

[5] S. Sen, S. K. Kumar, and P. Keblinski, Macromolecules **38**, 650 (2005).

[6] K. Kremer and G. S. Grest, J. Chem. Phys. **92**, 5057 (1990).

[7] R. Yamamoto and A. Onuki, J. Chem. Phys. **117**, 2359 (2002).

[8] R. B. Bird, R. C. Armstrong, and O. Hassager, *Dynamics of polymeric liquids* Vol. 1 (John Wiley and Sons, New York, 1987).

[9] R. G. Larson, *Constitutive equations for polymer melts and solutions* (Butterworths, Boston, 1988).

[10] M. Vladkov and J. L. Barrat, Macromol. Theory Simul. **15**, 252 (2006).